ELSEVIER

Nuclear Medicine and Biology 31 (2004) 165–171

NUCLEAR MEDICINE — AND — BIOLOGY

www.elsevier.com/locate/nucmedbio

Quantitative measurement of histamine H_1 receptors in human brains by PET and [^{11}C]doxepin

Hideki Mochizuki[a,b], Yuichi Kimura[b,*], Kenji Ishii[b], Keiichi Oda[b], Toru Sasaki[b], Manabu Tashiro[a], Kazuhiko Yanai[a], Kiichi Ishiwata[b]

[a]*Department of Pharmacology, Tohoku University School of Medicine, Sendai, Japan*
[b]*Positron Medical Center, Tokyo Metropolitan Institute of Gerontology, Tokyo, Japan*

Received 11 May 2003; received in revised form 4 August 2003; accepted 30 August 2003

Abstract

The aim of this study is to establish a method for quantitative measurement of histamine H_1 receptor (H1R) in human brain by PET and [^{11}C]doxepin ([^{11}C]DOX). The estimated parameters with a two-compartment model were stable for the initial values for parameter estimation but those with a three-compartment model were not. This finding suggests that the H1R measured by the [^{11}C]DOX and PET can be evaluated with a two-compartment model. © 2004 Elsevier Inc. All rights reserved.

Keywords: Compartment model; Histamine H_1 receptor; PET; [^{11}C]doxepin

1. Introduction

Histamine neurons are exclusively located in the tuberomammillary nucleus of hypothalamus, and diffusely project their fibers to almost all areas of brain. They are thought to be involved in the regulation of various physiological functions such as wakefulness and cognition through at least four histamine receptor subtypes: G protein coupled H_1 ($G_{q/11}$), H_2 (G_s), H_3 (G_i) and H_4 (G_i) [8,23,27,28]. H_1 and H_2 receptors are located at the postsynaptic sites of the histamine neurons, and H_3 receptors are functioning as an autoreceptor. H_3 receptor-activation inhibits the release of neural histamine. It was reported that impairments of cognition and motor functions and sedation were caused by H_1 antagonists [8]. Histamine H_1 receptors (H1R) are important for cortical activation as well as H_2 receptors [17,21]. The precise functions of H_4 receptor in brains have been scarcely understood since it was found recently. Antihistaminic drugs are often used to relieve allergies, coughs and colds, but they elicit sedation and affect cognition and behavior through the cortical inactivation [1,20,22]. Therefore, many studies have been carried out to develop antihistaminic drugs that do not penetrate the blood brain barrier (BBB). The blockade of H1Rs in brains is cause of sedation. Therefore, it is important to evaluate the occupancy of H1Rs by antihistamine in order to verify the side effects of antihistaminic drugs on the central nervous system (CNS). In vivo imaging techniques such as single photon emission computed tomography (SPECT) and positron emission tomography (PET) can provide a clear understanding of physiological processes in the human brain. Therefore, the therapeutic efficacies of drugs on the CNS have been extensively investigated in term of the receptor occupancy in the living human brain [4,24]. As for the H1R occupancy by antihistaminic drugs, PET with [^{11}C]doxepin ([^{11}C]DOX) has been used to evaluate objectively their possible side effects due to the penetration through BBB [26].

For quantitative PET measurement of receptor density, an appropriate model to describe the underlying kinetic of the individual radioligand should be developed because the model is different among the ligands used, even though their target receptor is the same [6,9]. Most of receptor imaging studies underwent the compartment model analysis with a nonlinear curve fitting algorithm to evaluate receptor density [7,9]. So far the evaluation of H1R density by [^{11}C]DOX and PET was performed by usually established methods such a graphical analysis with a three-compartment

* Corresponding author. Tel.: +81-3-3964-3241 ex.3506; fax: +81-3-3964-2188.
E-mail address: ukimura@ieee.org (Y. Kimura).

0969-8051/04/$ – see front matter © 2004 Elsevier Inc. All rights reserved.
doi:10.1016/j.nucmedbio.2003.08.010

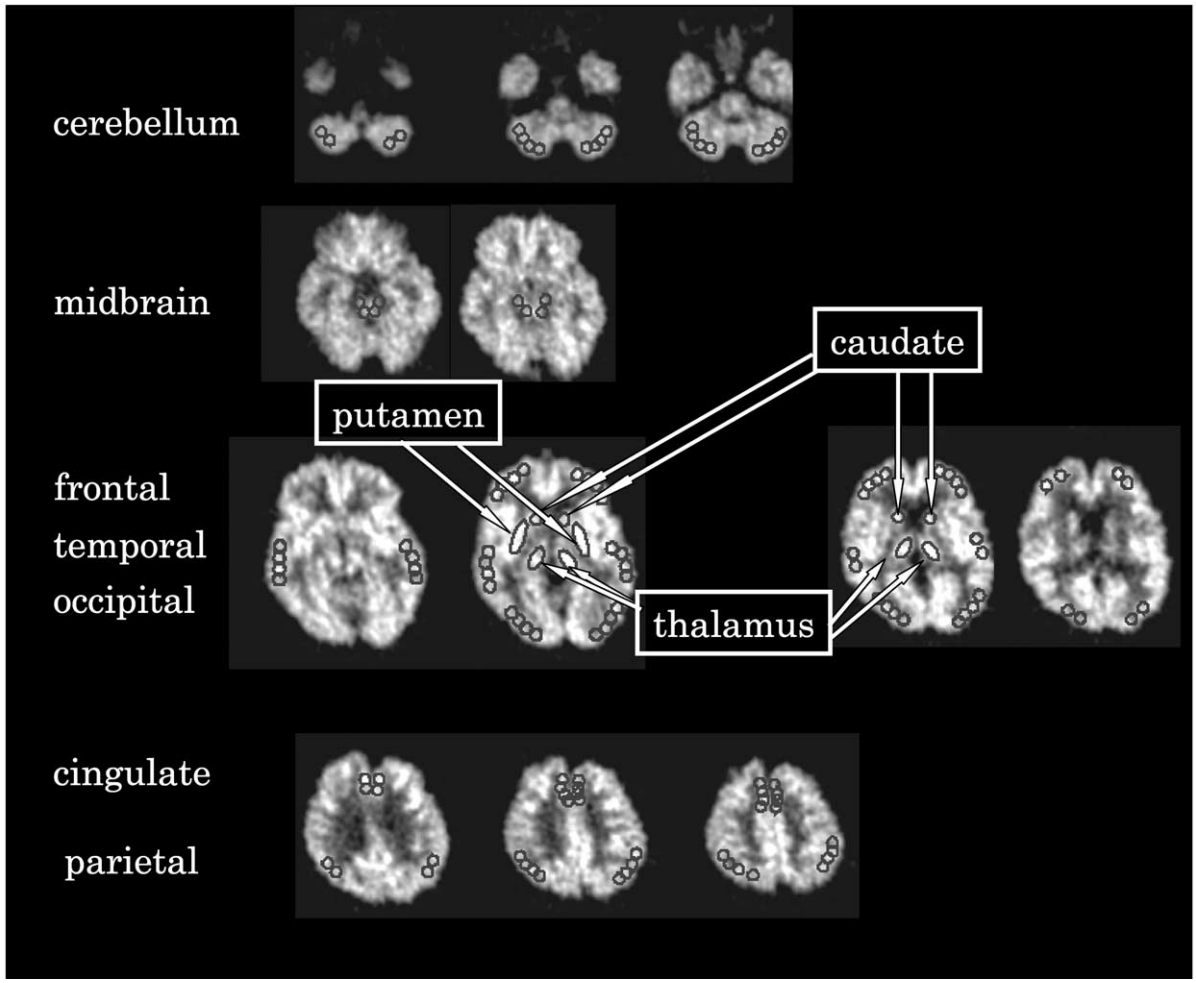

Fig. 1. The ROI placements: Several circles were placed to cover the cerebellum, frontal, parietal, temporal, occipital and cingulate cortices; and the thalamus, caudate, putamen and midbrain.

model [10] and a static image at the later phase [31]. However, the rationale of these analyses has not been verified yet. Thus, in this paper we investigated the applicability of two- and three-compartment models to the quantitative evaluation of H1Rs in human brains by using [^{11}C]DOX and PET.

2. Materials and methods

2.1. Subjects

Five healthy male volunteers, 21–27 years old, participated in this study. No subjects had any previous history of psychiatric disorders. No anatomical abnormalities were found in the MRI images. They were asked to abstain from medication a week before the study, and from tobacco, caffeine, grapefruit and beverages including grapefruit that modulate the concentration of antihistamines in plasma [15] on the experimental day. Written informed consent was obtained from the subjects. The study was approved by the respective Ethics Committees of the Tokyo Metropolitan Institute of Gerontology and of Tohoku University School of Medicine, and performed in compliance with relevant laws.

2.2. Radiosynthesis of [^{11}C]DOX

[^{11}C]DOX was synthesized by [^{11}C]methylation of the demethyl doxepin with [^{11}C]methyl triflate [11] with some modifications. Briefly, [^{11}C]methyl triflate was prepared as reported previously [12], then it was bubbled in 0.25 ml of acetone containing 0.25 mg of demethyl doxepin and 10 μl of 1 M NaOH at room temperature. Then, 1.3 ml of 0.1 M HCl/CH_3CN/50 mM $CH_3CO_2NH_4$ (50/22.5/27.5, v/v) was added to the reaction mixture and the solution was applied to high-performance liquid chromatography (HPLC): column, YMC-Pack ODS-A (10 mm inner diameter $\times$ 250 mm length, YMC Co., Kyoto, Japan); eluent, CH_3CN/50 mM $CH_3CO_2NH_4$ (45/55, v/v); and flow rate, 5 ml/min. A fraction containing the [^{11}C]DOX was collected. After adding 50 μl of 250 mg/ml ascorbate, the fraction was evaporated to dryness, and the residue was dissolved in a physiological

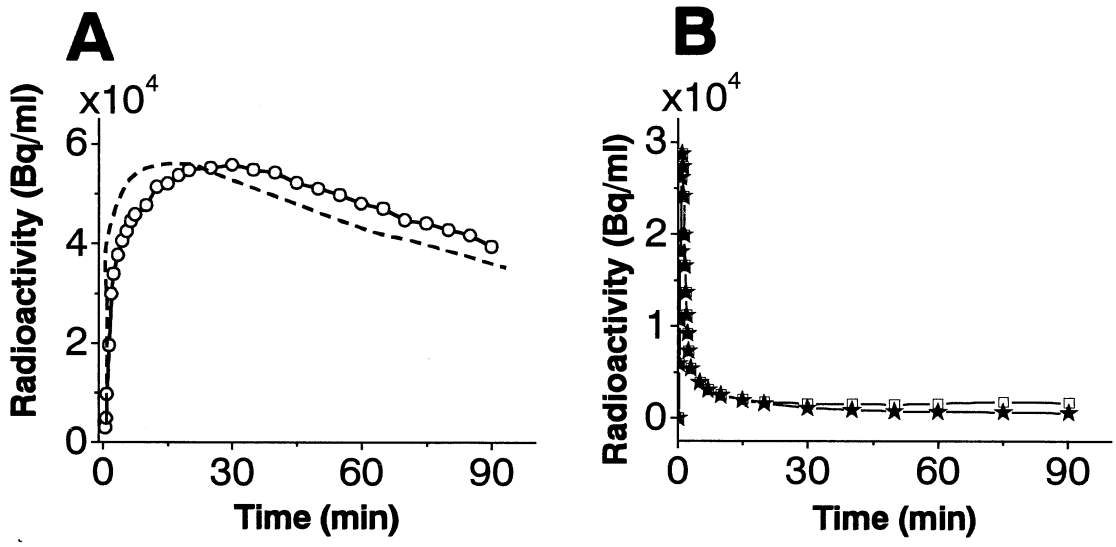

Fig. 2. Typical time-activity curves of whole–brain (tTAC) after intravenous injection of [^{11}C]doxepin into a subject: circle, tTAC measured; solid line, tTACs estimated with the two-compartment model; and dashed line, tTAC estimated with three-compartment model (A) and time-activity curves of plasma (pTAC): square. pTAC measured; and star, pTAC metabolite-corrected (B).

saline solution. The [^{11}C]DOX solution was filtered through a 0.22 μm membrane filter. The radiochemical yields was 1930 ± 620 MBq, and the specific activity was 84 ± 43 TBq/mmol. The radiochemical purity was over 99%, and neither ^{11}C-methylated DOX [11] nor starting materials were included.

2.3. Pet measurements

Dynamic scans in two-dimensional mode were performed using Headtome-V (Shimadzu Co., Kyoto, Japan), which acquires 63 slices having 128-by-128 voxels each at transverse resolutions of 4.5 mm full width of half maximum (FWHM) and at axial resolution of 5.8 mm FWHM. PET images were reconstructed with a filtered backprojection algorithm. Corrections were applied to dead time, detector uniformity and photon attenuation. The frame arrangement was: 10 sec × 6 frames, 30 sec × 3 frames, 60 sec × 5 frames, 2.5 min × 5 frames and 5 min × 14 frames, totally 90 min. The injected radioactivity dose of [^{11}C]DOX was 493 ± 109 MBq and the cold mass 23 ± 16 (nmol) (mean ± SD). Arterial blood was sampled every 10 sec for the first 150 sec post-injection, and afterward at 3, 5, 7, 10, 15, 20, 30, 40, 50, 60, 75 and 90 min post-injection.

2.4. Measurement of labeled metabolites in plasma

Metabolite analysis was carried out using six plasma samples obtained 3, 10, 20, 30, 40 and 60 min after the injection [13] with a slight modification. The plasma samples were treated with CH_3CN containing trichloroacetic acid, and divided into the acid-soluble and acid-precipitable fractions. Over 96% of the total activity was recovered in the acid-soluble fraction. The acid-soluble fraction was analyzed by HPLC: column, Nova-pak C18 equipped with an RCM 8 x 10 compression module (Waters); eluent, CH_3CN/50 mM $CH_3CO_2NH_4$ (45/55, v/v); flow rate, 2 ml/min. The recovery of the radioactivity in the HPLC analysis was essentially quantitative. Percentages of the unchanged [^{11}C]DOX were 98.9 ± 0.5, 97.9 ± 1.5, 92.0 ± 3.9, 79.5 ± 8.6, 71.3 ± 7.6 and 51.6 ± 8.9 at 3, 10, 20, 30, 40 and 60 min, respectively.

2.5. Data analysis

Regions of interest (ROIs) were drawn on the frontal, temporal, occipital, parietal and cingulate cortices and the thalamus, caudate nucleus, putamen, cerebellum and midbrain to derive average time activity curves in the tissues (tTACs) (Fig. 1).

Usually, the receptor density can be evaluated as binding potential ($BP = k_3/k_4$) in the kinetic analysis using a three-compartment model proposed by Mintun [19]. If an equilibrium state is accomplished quickly, the receptor density can be represented using a distribution volume ($DV = K_1/k_2$) [16]. Dynamics of the ligands are different individually [26]. That is, an appropriate model for the evaluation of the receptor density depends on not only the receptor but also the ligand used. Therefore, two- and three- compartment models were applied to the kinetic analysis for [^{11}C]DOX in terms of stability of estimates against the initial values for parameter estimation because non-linear curve fittings could require the stability. To investigate the stability of model estimation, initial values of K_1, k_2, k_3, and k_4 were varied from 0.1 to 0.4, respectively. Bv was fixed 0.

The models were estimated with ordinary nonlinear curve fitting algorithm of Newton's method [3]. Delay between tTAC and the plasma time activity curve (pTAC) was

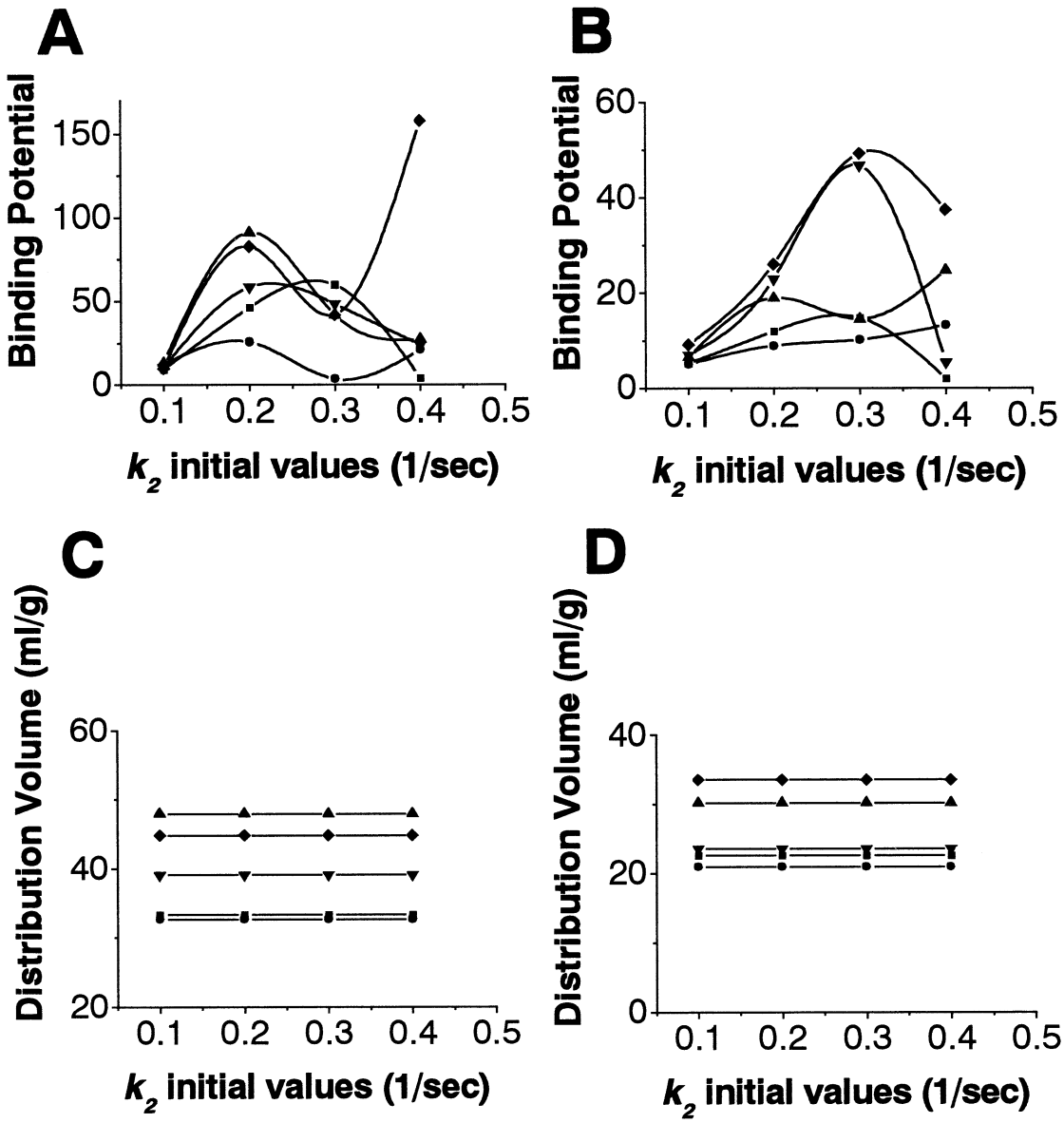

Fig. 3. Stability between initial value for parameter estimation and estimate. Upper (A and B) and lower (C and D) denote the dependency in the three- and two-compartment model, respectively. The left column (A and C) originated from the right cingulate cortex being rich in histamine H_1 receptor (H1Rs), and the right column (B and D) from the right cerebellum being poor in H1Rs. Results of all five subjects were superimposed.

estimated using an averaged tTAC of the whole-brain and it was assumed to be common among subjects. In addition, Akaike information criterion (AIC) was used to identify which model fit better for the averaged tTAC in the whole brain [2].

3. Results

3.1. Comparison of two- and three-compartment models

Fig. 2 shows the estimated TAC in a whole-brain in the two- and three-compartment model (Fig. 2A) and pTACs for total radioactivity and unmetabolized [^{11}C]DOX (Fig. 2B).

The dependency of BP or DV for an initial value is shown in Fig. 3. In a three-compartment model, BP is largely altered in both the H1R-rich cingulate cortex and H1R-poor cerebellum. In the two-compartment model, DV is much more stable regardless of the initial guess. These findings were common for all of parameters. In addition, AICs in the two-compartment model were smaller in all regions than those in the three-compartment model. A typical AIC was 421 for a two-compartment model and 603 for a three-compartment model.

3.2. Distribution volume in each brain region

DV in 10 brain regions was estimated with a two-compartment model. DV in each brain region is summarized in

Table 1
Distribution volume (DV) observed in the present study and histamine, H_1 receptor (H1R) density in autopsied human brains

Brain areas	Present PET study DV (ml/g)	Post-mortem brain studies Histamine H_1 receptor density (pmol/g)		
		Chang [5]	Kanba [14]*	Yanai [30]
frontal cortex	37	4.3	19.1	3.6
temporal cortex	40	3.4	23.5	3.3
parietal cortex	37	4	16.6	
occipital cortex	32	1.8	13.2	1.8
cingulate cortex	37	3.8	22.3	
thalamus	35	0.9	4.3	1
caudate nucleus	34	1.3	5.3	
putamen	36	0.9	4.4	
midbrain	27		2.2	
cerebellum	26	0.4	1.6	0.3

* Fourth column: we calculated H1R density with the H1R density in the hypothalamus (7 nmol/g) and % of hypothalamus in each brain region reported by Kanba et al.

Table 1 with the previous reports of H1R density in autopsy studies of the human brain [5,14,29].

The DV had a good correlation with the H1R densities in the cortical regions (r = 0.91), while a less correlation was found when taking account of data in all brain regions (r = 0.73) (Fig. 4).

Since the cerebellum has a very low density of H1Rs (Table 1), it is reasonably considered that the DV in the cerebellum corresponds to that reflecting the non-specific binding of [^{11}C]DOX in the brain. Therefore, the difference between each DV and cerebellar DV reflects the specific binding of [^{11}C]DOX in each region. The subtracted DVs in the other regions are shown in Fig. 5.

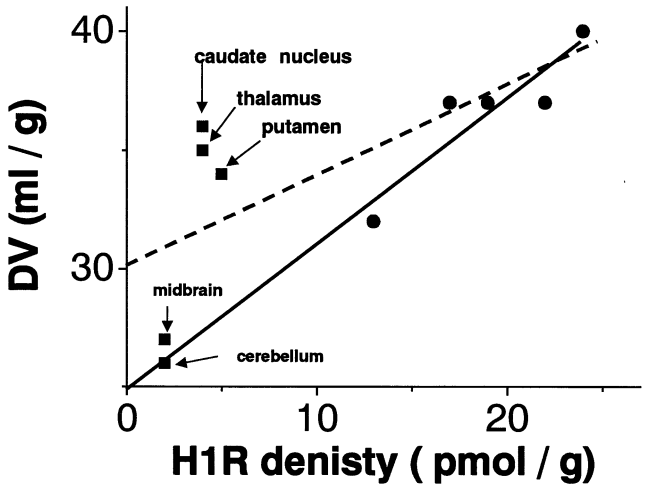

Fig. 4. The relationship between the DV of [^{11}C]DOX obtained in the present PET study and H1R density measured by using [^{3}H]DOX in the autopsy study [14]. Circles show five cortical regions. Squares show the thalamus, caudate nucleus, putamen, midbrain and cerebellum. Dashed line is the linear regression with all brain regions (Y = 0.4*X + 30, r = 0.74). Solid line is the linear regression with the five cortical regions (Y = 0.6*X + 25, r = 0.91). The discrepancy between the cortical and subcortical regions would be probably due to the unevenness of the non-specific bindings among these structures.

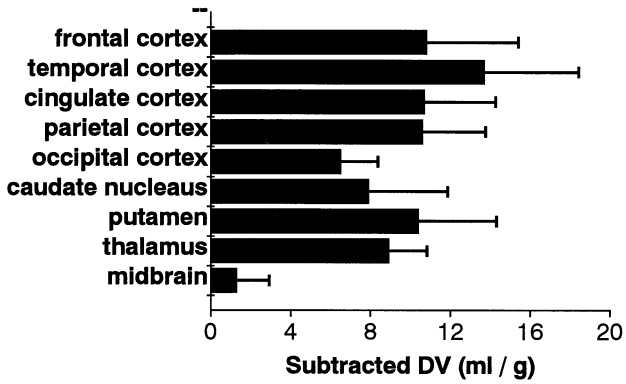

Fig. 5. The specific distribution volume (DV) of [^{11}C] DOX in the human brain. The specific DV was determined by the difference between DV in each brain region and that in the cerebellum, and expressed the mean ± SD (n = 5).

4. Discussion

4.1. Determination of compartment model

A compartment model for receptor analysis should be determined according to the behavior of radiopharmaceutical in the target organs. Usually the behavior is described with a three-compartment model and a binding potential [19]. If there is only a low level of free and non-specifically bound ligands in tissue and if rapid equilibration occurs between a free and non-specifically bound compartment and a specifically bound compartment, a two-compartment model is suitable for kinetic analysis [16]. In this study, the selection was settled on the point of view of stability in the parameter estimation and from the information available in the measured tTAC. In this case, the three-compartment model did not give stable estimates. BP fluctuated greatly with the change of initial values for K1, k2, k3 and k4 (Figs. 3A and 3B). On the other hand, a stable DV could be obtained regardless of the initial values in the two-compartment model (Figs. 3C and 3D). It means that the free [^{11}C]DOX pool is negligible and the free radioligand is indistinguishable from the bound radioligand pool in the three-compartment model.

The validity of the two models was also evaluated by AIC. The AIC of the two-compartment model was always smaller than that of the three-compartment model. The model with the smaller AIC value is more valid to describe the behavior of radioligand in the brain. Thus, our statistical criterion also indicates that the two-compartment model is more suitable than the three-compartment model for quantitative analysis of the [^{11}C]DOX binding to H1Rs if nonlinear curve fitting is used for calculation.

For quantitative analysis we used the metabolite-cor-

rected pTAC as an input function. We assumed that free and non-specifically bound ligands are present in a rapid equilibrium state. Therefore, in the metabolite analysis the plasma was treated with TCA in acetonitril solution to recover quantitatively both free and non-specifically bound radioactivities.

4.2. Distribution volume in the brain

As shown in Table 1, DV values of [^{11}C]DOX in the temporal, frontal and cingulate cortices were larger than that in the occipital cortex in this study. The DV of [^{11}C]DOX reflecting both specific and non-specific binding in these cortical regions, was proportional well to the H1R density measured in vitro by using [^{3}H]doxepin (Fig. 4). Because the cerebellar H1R density was negligibly low compared to the cortical densities in the post-mortem brain studies [5,14,30], the DV in the cerebellum is reasonably assumed to be the free and non-specific bound pool of [^{11}C]DOX in the brain. Thus, the specific DV reflecting the specific binding of [^{11}C]DOX in the cortical regions can be evaluated by subtracting the DV in the cerebellum from those in the cortical regions. On the other hand, DVs in the thalamus, caudate nucleus and putamen were similar to those in the cortices, though the H1R densities in the subcortical region were lower than those in the cortices in post-mortem studies [5,14,29] (Table 1). The correlation between the DVs and the reported H1R densities in all subcortical brain regions deviated significantly from the expected values compared to those in the cortices, suggesting that DVs in the thalamus and the striatum would not reflect the H1R densities exactly. We estimated DV in each brain region with tTAC obtained by the ROI placed on the gray matter referencing to the MRI image of each subject. Thus, the ROI placement would not be a cause of the discrepancy between the present in vivo and the previous in vitro studies. The competition between [^{11}C]DOX and endogenous histamine would be almost same in the brain, since projection of histaminergic neurons is almost uniform in the brain. One reason for the discrepancy could be the higher non-specific binding in the thalamus and striatum [18]. Yanai et al. measured specific binding and non-specific binding with the autopsied human brain using [^{3}H]pyrilamine. They found that non-specific binding in the thalamus and the striatum was 212% and 125% of the cortex, respectively [30]. We also confirmed that these regions showed the higher non-specific binding of [^{11}C]DOX than the cortical regions by the blocking study with d-chlorpheniramine [31]. In the in vitro ligand-receptor binding studies, the H1R density was defined as the radioactivity specifically bound after subtracting the non-specific binding determined in the presence of a large amount of antihistaminic drug [5,14,30], while the specific DVs were determined by subtracting the DV in the cerebellum from that in each region. The subtraction would not be able to eliminate properly the binding sites except for H1Rs in the thalamus, caudate nucleus and putamen.

In this paper, it was found that a two-compartment model is suitable for quantitative PET measurement of H1Rs using [^{11}C]DOX and a non-linear curve fitting. The [^{11}C]DOX and PET gives reliable information on the H1Rs in cortical regions because it has limited potential in subcortical regions such as the striatum and thalamus, possibly because of nonspecific binding [24].

Acknowledgments

This work was partly supported by Grants-in-Aid from the Ministry of Education, Culture, Sports, Science, and Technology, and from the Ministry of Health, Labor and Welfare, Japan. The authors thank the volunteers in the PET measurement, Ms. Miyoko Ando for care of subjects and Mr. Kazunori Kawamura for the preparation of [^{11}C]DOX.

References

[1] Adelberg BR. Sedation and performance issues in the treatment of allergic conditions. Arch Int Med 1997;157:494–500.
[2] Akaike H. A new look at the statistical model identification. IEEE Automatic Control A 1974;C19:716–22.
[3] Borse GJ. Numerical Methods with MATLAB. International Stamford: Thomson Publishing Inc.; 1997, p. 177-188.
[4] Bressan RA, Erlandsson K, Jones HM, Mulligan RS, Ell PJ, Pilowsky LS. Optimizing limbic selective D2/D3 receptor occupancy by risperidone: a [^{123} I]-epidepride SPET study. J Clin Psychopharmacol 2003;23(1):5–14.
[5] Chang RSL, Tran VT, Snyder SH. Heterogeneity of histamine H1-receptors: Specific variations in [^{3}H]mepyramine binding of brain membranes. J Neurochem 1979;32:1653–63.
[6] Chugani DC, Muzik O, Chakraborty P, Mangner T, Chugani HT. Human brain serotonin synthesis capacity measured in vivo with alpha-[C-11]methyl-L-tryptophan. Synapse 1998;28(1):33–43.
[7] DaSilva JN, Lourenco CM, Meyer JH, Hussey D, Potter WZ, Houle S. Imaging cAMP-specific phosphodiesterase-4 in human brain with R-[^{11} C]rolipram and positron emission tomography. Eur J Nucl Med Mol Imaging 2002;29(12):1680–3.
[8] Haas H, Panula P. The role of histamine and the tuberomamillary nucleus in the nervous system. Nat Rev Neurosci 2003;4(2):121–30.
[9] Hagberg GE, Torstenson R, Marteinsdottir I, Fredrikson M, Langstrom B, Blomqvist G. Kinetic compartment modeling of [^{11}C]-5-hydroxy-L-tryptophan for positron emission tomography assessment of serotonin synthesis in human brain. J Cereb Blood Flow Metab 2002;22(11):1352–66.
[10] Higuchi M, Yanai K, Okamura N, Meguro K, Arai H, Itoh M, Iwata R, Ido T, Watanabe T, sasaki H. Histamine H_1 receptors in patients with Alzheimer's disease assessed by positron emission tomography. Neuroscience 2000;99:721–9.
[11] Iwata R, Pascali C, Bogni A, Yanai K, Kato M, Ido T, Ishiwata K. A combined loop-SPE method for the automated preparation of [^{11}C]doxepin. J Label Compd Radiopharm 2002;45:271–80.
[12] Ishiwata K, Koyanagi Y, Saitoh T, Taguchi K, Toda J, Sano T, Senda M. Effects of single and repeated administration of 1,2,3,4-tetrahydroisoquinoline analogs on the binding of [^{11}C]raclopride to dopamine D_2 receptors in the mouse brain. J Neural Transm 2001;108: 1111–25.
[13] Ishiwata K, Itou T, Ohyama M, Yamada T, Mishina M, Ishii K, Nariai T, Sasaki T, Oda K, toyama H, Senda M. Metabolite analysis

of [11C]flumazenil in human plasma: assessment as the standardized value for quantitative PET studies. Ann Nucl Med 1998;12:55–9.
[14] Kanba S, Richelson E. Histamine H_1 receptors in human brain labeled with [3 H]doxepin. Brain Res 1984;304:1–7.
[15] Kane GC, Lipsky JJ. Drug-grapefruit juice interactions. Mayo Clin Proc 2000;75:933–42.
[16] Koeppe RA, Holthoff VA, Frey KA, Kilbourn MR, Kuhl DE. Compartmental analysis of [11C]flumazenil kinetics for the estimation of ligand transport rate and receptor distribution using positron emission tomography. J Cereb Blood Flow Metab 1991;11:735–44.
[17] Lopez-Garcia JA, Ramis C, Nicolau MC, alemany G, Planas B, Rial R. Histaminergic drugs in the rat caudate nucleus: effects on learned helplessness. Pharmacol Biochem Behav 1993;45(2):275–82.
[18] Martinez-Mir MI, Pollard H, Moreau J, Arrang JM, Ruat M, Traiffort E, Schwartz JC, Palacios JM. Three histamine receptors (H1, H2 and H3) visualized in the brain of human and non-human primates. Brain Res 1990;526(2):322–7.
[19] Mintun MA, Raichle ME, Kilbourn MR, Wooten GF, Welch MJ. A quantitative model for the in vivo assessment of drug binding sites with positron emission tomography. Ann Neurol 1984;15:217–227.
[20] Mochizuki H, Tashiro M, Tagawa M, Kano M, Itoh M, Okamura N, Watanabe T, Yanai K. The effects of a sedative antihistamine, d-chlorpheniramine, on visuomotor spatial discrimination and regional brain activity as measured by positron emission tomography (PET). Hum Psychopharmacol 2002;17(8):413–8.
[21] Moscati RM, Moore GP. Comparison of cimetidine and diphenhydramine in the treatment of acute urticaria. Ann Emerg Med 1990; 19(1):12–5.
[22] Nicholson AN. Central effects of H1 and H2 antihistamines. Aviat Space Environ Med 1985;56:293–8.
[23] Parmentier R, Ohtsu H, Djebbara-Hannas Z, Valatx JL, Watanabe T, Lin JS. Anatomical, physiological, and pharmacological characteristics of histidine decarboxylase knock-out mice: evidence for the role of brain histamine in behavioral and sleep-wake control. J Neurosci 2002;22(17):7695–711.
[24] Schmitt GJ, Meisenzahl EM, Dresel S, tatsch K, Rossmuller B, Frodl T, Preuss UW, Hahn K, Moller HJ. Striatal dopamine D2 receptor binding of risperidone in schizophrenic patients as assessed by 123I-iodobenzamide SPECT: a comparative study with olanzapine. J Psychopharmacol 2002;16(3):200–6.
[25] Szabo Z, McCann UD, Wilson AA, Scheffel U, Owonikoko T, Mathews WB, Ravert HT, Hilton J, Dannals RF, Ricaurte GA. Comparison of (+)-11 C-McN5652 and 11 C-DASB as serotonin transporter radioligands under various experimental conditions. J Nucl Med 2002;43(5):678–92.
[26] Tagawa M, Kano M, Okamura N, Higuchi M, Matsuda M, Mizuki Y, Arai H, Iwata R, Fujii T, Komemushi S, Ido T, Itoh M, Sasaki H, Watanabe T, Yanai K. Neuroimaging of histamine H1-receptor occupancy in human brain by positron emission tomography (PET): a comparative study of ebastine, a second-generation antihistamine, and (+)-chlorpheniramine, a classical antihistamine. Br J Clin Pharmacol 2001;2:501–509.
[27] Watanabe T, Taguchi Y, Shiosaka S, Tanaka J, Kubota H, Terano Y, Tohyama M, Wada H. Distribution of histaminergic neuron system in the central nervous system of rats; a fluorescent immunohistochemical analysis with histidine decarboxylase as a marker. Brain Res 1984;295:13–25.
[28] Watanabe T, Yanai K. Studies on functional roles of the histaminergic neuron system by using pharmacological agents, knockout mice and positron emission tomography. Tohoku J Exp Med 2001;195: 197–217.
[29] Yanai K, Watanabe T, Yokoyama H, Hatazawa J, Iwata R, Ishiwata K, Meguro K, Itoh M, Takahashi T, Ido T. Mapping of histamine H_1 receptors in the human brain using [11C]pyrilamine and positron emission tomography. J Neurochem 1992;59:128–36.
[30] Yanai K, Watanabe T, Meguro K, Yokoyama H, Sato I, Sasano H, Itoh M, Iwata R, Takahashi T, Ido T. Age-dependent decrease in histamine H_1 receptor in human brains revealed by PET. Neuroreport 1992;3(5):433–6.
[31] Yanai K, Watanabe T, Yokoyama H, Meguro K, Hatazawa J, Itoh M, Iwata R, Ishiwata K, Takahashi T, Ido T. Histamine H_1 receptors in human brain visualized in vivo by [11 C]doxepin and positron emission tomography. Neurosci Lett 1992;137:1457.